

Glue-free tuning fork shear-force microscope

P. Mühlischlegel, J. Toquant, D. W. Pohl, and B. Hecht^{a)}

Nano-Optics group, National Center of Competence for Research in Nanoscale Science, Institute of Physics, University of Basel, Klingelbergstrasse 82, CH-4056 Basel, Switzerland

(Received 17 October 2005; accepted 14 December 2005; published online 25 January 2006)

A scanning near-field optical microscope without any glued parts is described. Key elements are the optical fiber probe/tuning fork junction and the piezotube scanner assembly. In both cases, fixation is achieved by means of controlled pressure and elastic deformation. The avoidance of glued connections was found to improve the Q factor of the shear-force sensor as well as to facilitate the replacement of the fiber probe and other parts of the scanner head. We present approach curves and shear-force images that demonstrate the performance and stability of the system. © 2006 American Institute of Physics. [DOI: 10.1063/1.2165548]

Piezoelectric shear-force sensors are widely used for probe-sample distance control in scanning near-field optical microscopy^{1–7} (SNOM) and other scanning probe techniques (see Ref. 8 for further reference). In SNOM the optical probe is usually attached to a quartz tuning fork (TF), of the type used in watches. The interaction of the probe with the surface induces a shift of the TF's resonance frequency. This shift or the resulting impedance change can be used for distance control by means of a feedback mechanism acting on the so-called z piezo, usually a piezoelectric ceramic tube. The TF is excited either mechanically by a piezoelectric element, or electrically by a driving voltage applied directly to the TF.² The stiffness and fragility of fiber SNOM probes require a sensitive and fast feedback to prevent probes from crashing during approach and scanning. Therefore a sensor with high-quality factor (Q), in combination with a phase-locked loop (PLL) feedback system, is desirable.

The standard method of connecting a fiber probe to the TF is gluing with epoxy.^{1,4,7} This process is somewhat problematic since the adhesive tends to form a thin cushion between fiber and TF. The latter forms a “soft” connection because the elastic properties of quartz and epoxy are widely different, the elastic modulus of the latter being 20 times smaller than that of quartz (see, e.g., Ref. 9) and also having appreciable loss at the typical tuning fork frequencies (=32 kHz). The losses generate damping and result in reduced Q -factor values [e.g., ~ 1000 (Ref. 1)]. To minimize the resulting damping, the gluing process has to be controlled carefully which requires considerable skill and experience. Once glued, a probe cannot be removed easily, e.g., for characterization; neither can a poorly glued probe be re-adjusted after curing of the epoxy.

To circumvent probe gluing, mechanical fixation by clamping the fiber probe between the two arms of a TF (Ref. 5) or connecting the probe to a homebuilt piezoceramic TF (Ref. 6) has been suggested. The present scheme is based on the same principle; however, it relies on an improved mechanical design. It provides adjustable Q factors as high as ~ 4000 , resulting in high force sensitivity and in conjunction

with a PLL short feedback response time. The very simple compact implementation allows for particularly fast, easy, and reproducible probe exchange.

The elimination of glued parts from the z piezo results in similar advantages as described for the shear-force sensor. Therefore the piezoceramic tube used as z piezo is mounted between two adaptors kept together by means of an appropriately designed screw instead of an adhesive. The main improvements here are the ease of mounting and replacement, the well-defined mechanical parameters, and the higher Q .

Figure 1 shows the relevant parts of the SNOM head. Fixation of probe holder base plate (BP) and z piezotube (PT) is illustrated in Fig. 1(a). Screw S (steel) exerts a compression force on the assembly that is adjusted by means of a sensitive torque wrench. Torques in the range of 3–8 cN m were found to provide stable fixation without damage of the brittle piezoceramic material (PZT Staveley EBL3, length = 35 mm, $D=6.25$ mm, and $w=0.5$ mm). The electromechanical response of the PT is influenced marginally only by the screw. Since the elastic moduli of steel and standard piezoceramics are roughly the same, the longitudinal (z direction) piezoelectric expansion is reduced in proportion to the ratio of the cross-sectional areas which is $<17\%$, hence irrelevant in most applications. With respect to bending (lateral scanning), the influence is completely negligible since here the area moments of inertia are the relevant parameters which differ by more than three orders of magnitude. Figure 1(b) displays the mechanical resonances of the PT, measured with a spectrum analyzer, the excitation voltage being applied to one pair of the quadrant electrodes of the PT, and the signal being picked up from the other pair. The measurement was performed for two different torques applied to screw S and for a conventionally glued z piezo. Apparently, the low-frequency resonances of the glued piezotube move to higher frequencies for the unglued, clamped piezo.

TF and the fiber probe with removed coating are mounted in separate blocks B1 and B2 [Figs. 1(c) and 1(d)] such that the fiber is pressed against one prong of the slightly tilted TF near its end. The blocks are screwed to the insulating BP. The relative position of the blocks determines the position H of mechanical contact between TF and fiber and

^{a)}Electronic mail: bert.hecht@nano-optics.ch

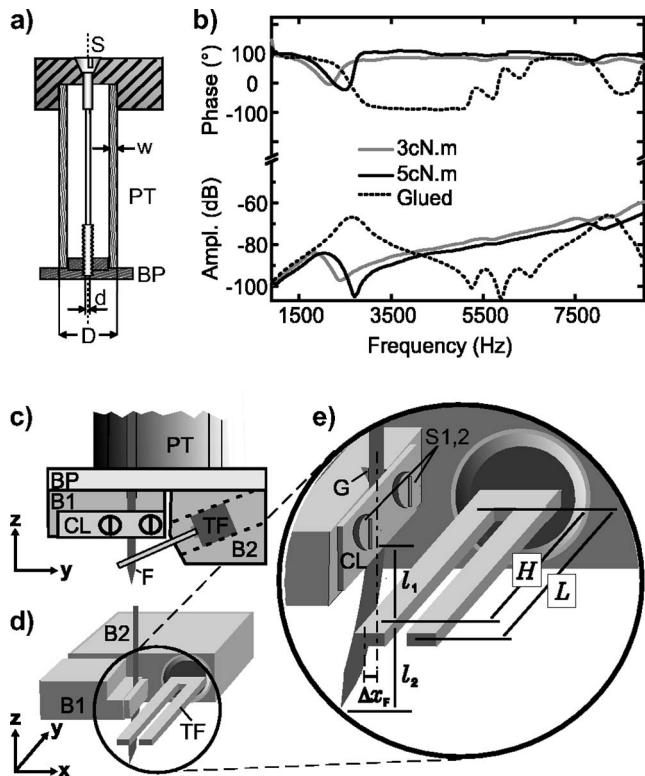


FIG. 1. Scanner assembly and tuning fork mount. (a) Sketch of the clamped piezotube (PT). S : fixation screw, D : PT outer diameter, w : width of PT walls, and d : diameter of the screw. (b) Resonance curves of the clamped piezotube for different torques exerted on the screw compared to a glued piezotube [top phases shift] bottom: normalized amplitudes]. (c)–(e) Sketch of the tuning fork mount. (c) (side view) PT: piezotube, BP: insulating base plate, TF: tuning fork, F : fiber, CL: clamp, B1: block with clamp and screws for fiber fixation, and B2: block with incorporated TF. (d) Rotated view without PT and BP. (e) Magnification of the indicated position in (d). G : groove for fiber guidance, $S1,2$: screws for clamp fixation, Δx_F : fiber bending amplitude, l_1 : distance between fixed fiber end and TF, l_2 : length of free fiber end, H : distance between TF base and fiber, and L : TF length.

the amount of fiber bending Δx_F that we adjusted to $\approx 100 \mu\text{m}$ [Fig. 1(e)]. Bending of the fiber results in a force $F = \Delta x_F k_F$ acting on the TF. The spring constant of the slightly bent cylindrical fiber, anchored on one side, was calculated as¹⁰ $k_F = (3\pi ER^4)/(4l_1^3) (\approx 600 \text{ N/m})$. Here E , R , and l_1 are Young's modulus, radius, and length of the bent part of the fiber, respectively. With $E = 6 \times 10^{10} \text{ N/m}^2$ (SiO_2),¹⁰ $R = 62.5 \mu\text{m}$, and $l_1 = 1.5 \text{ mm}$ [Fig. 1(e)], the total force exerted by the fiber on the TF amounts to 0.06 N. For stable operation it is instrumental that the probe follows the motion of the tuning fork prong without loosing contact at any moment in time during the tuning fork oscillation. The acceleration $\ddot{x}_F(l_1)$ of the free fiber towards the prong hence has to be larger than the maximum acceleration $\ddot{x}_T(H)$ of the TF prong during vibration. To calculate \ddot{x}_j ; $j \in \{F, T\}$ the solution to the equation of motion of a vibrating lever (fiber or TF prong) has to be separated:¹⁰ $x_j(z, t) = x_j(z) \exp(i\omega_j t)$. The maximum acceleration for the fundamental resonance frequency ω_j follows as

$$|\ddot{x}_j(z)|_{\text{max}} = \omega_j^2 |\Delta x_j(z)|, \quad (1)$$

where $|\Delta x_j(z)|$ is the maximum bending amplitude of the respective levels. The fundamental resonance frequency of an oscillating fiber with a circular cross section fixed on one

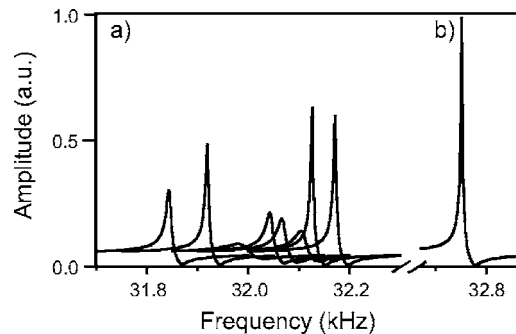


FIG. 2. (a) Resonance curves for a repeatedly mounted fiber. (b) Resonance of the freely oscillating tuning fork.

end is¹⁰ $\omega_F = (1.76\sqrt{E/\rho})R/l^2 \approx 2\pi(15 \text{ kHz})$, where $\rho = 2.2 \times 10^3 \text{ kg/m}^3$ is the specific mass density of SiO_2 ,¹⁰ and $l = l_1 + l_2 \approx 2.5 \text{ mm}$ is the length of the oscillating free fiber [Fig. 1(e)]. This results in $|\ddot{x}_F(l_1)|_{\text{max}} \approx 8 \times 10^5 \text{ m/s}^2$. The vibration amplitude $|\Delta x_T(H)|$ of the free TF was estimated from the driving voltage $V_D = 0.8 \text{ mV}$ and resulting current signal $I_{\text{max}} \approx 1.4 \text{ nA}$ of our TF [length: $L = 4.0 \text{ mm}$, thickness: $T = 0.63 \text{ mm}$, width: $W = 0.35 \text{ mm}$, resonance frequency: $\omega_T = 2\pi(32768 \text{ Hz})$, and static spring constant: $k_{\text{stat}} = 26.9 \mu\text{N/nm}$] by comparison with data for a TF of a similar type² where $V_D = 2 \text{ mV}$, $I_{\text{max}} = 2.9 \text{ nA}$ and a vibration amplitude of 0.4 nm were measured. This yields $|\Delta x_T(H)| < 1 \text{ nm}$ and hence $|\ddot{x}_T(H)|_{\text{max}} < 40 \text{ m/s}^2$. Thus $|\ddot{x}_F(l_1)|_{\text{max}} \gg |\ddot{x}_T(H)|_{\text{max}}$ which ensures safe contact between fiber and TF.

The ratio $R = L/H$ between total TF length L and fiber mounting position H [Fig. 1(e)] shows a strong influence on the Q factor of the coupled system fiber/TF, also reported by Crottini *et al.*⁷ The position H can be tuned to optimum condition in our arrangement by appropriate adjustment of B1 and B2 with respect to BP [Figs. 1(c) and 1(d)]. Once B1 and B2 are fixed in a favorable position, the probe (fiber) can be replaced within a few minutes by loosening screws ($S1,2$). Clamp CL opens up such that the old fiber can easily be pulled out from groove G and be replaced by a fresh one [Fig. 1(e)].

To characterize the influence of the fiber on the TF, a fiber was mounted and unmounted ten times and the resonance was measured each time (Fig. 2). An average resonance frequency $\bar{f}_0 = 32047 \pm 250 \text{ Hz}$ and an average $\bar{Q} = 2032 \pm 1612$ factor were determined. Since the static spring constant k_{stat} of the TF is hardly altered by the fiber, we assign the observed shift ($\approx -700 \text{ Hz}$) of the resonance for the coupled fiber/TF system with respect to the free TF [Fig. 2(b)] and to the increase in effective mass m_0 due to the attached fiber. The scattering of the data is attributed to the uncertainty in length l_2 . The deviation in Q is due to slight variations in clamp fixation [Fig. 1(e)].

Samples were mounted on a regulated x - y scan stage (Physik Instrumente, P-733) for imaging. The TF current signal was preamplified and converted to an oscillating voltage by a current-to-voltage amplifier (amplification factor: 2×10^7). Gap width feedback control was established by means of a phase-locked loop (PLL, Nanosurf AG) and the preamplified TF signal. The use of a PLL reduces the response time of the feedback system.⁴ Fiber probes were pro-

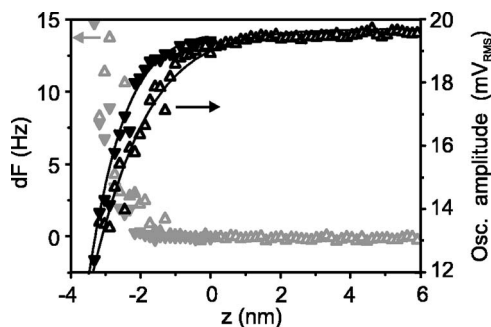


FIG. 3. Approach curve towards a SiO_2 surface. Voltage oscillation amplitude (black) and frequency shift dF (gray) are recorded during approach (filled triangles) and retract (open triangles) starting from position $z=0$.

duced by tube etching,¹¹ followed by hot sulfuric acid (96%) removal of the fiber coating on the tip end side.

Approach curves and shear-force images of a SiO_2 calibration sample were recorded to demonstrate the functionality and robustness of the glue-free TF shear-force microscope. Figure 3 shows the damping of the voltage oscillation amplitude and the frequency shift when the tip is approached to and retracted from the SiO_2 surface. First the z piezo approaches the tip to the surface. The active feedback system stopped the approach when gentle shear-force contact was established (amplitude damping $<3\%$). From this point on ($z=0$ in Fig. 3) the feedback system was turned off and further approach was started. Retraction was triggered when the oscillation amplitude reached a predefined lower limit. The deviation between approach and retraction curves is caused by hysteresis of the z piezo. The fit curves were obtained from a shear-force model¹² describing the damping of the resonance amplitude for an approaching tip. The amplitude drops within 3 nm to 70% of its undisturbed value, comparable to the data reported by others.^{6,7} The resonance frequency was found to increase simultaneously with the damping in amplitude.

Figure 4(a) depicts a shear-force image of a SiO_2 calibration sample, consisting of a two-dimensional lattice of inverted square pyramids with 200 nm pitch etched into a silicon chip. Figures 4(b)–4(d) show the data recorded along the line marked in Fig. 4(a), topography, the voltage oscillation amplitude, and the frequency shift. At a scan speed of $1 \mu\text{m/s}$ the topography profile is slightly asymmetric due to the feedback response time [Fig. 4(b)], however, the amplitude never dropped below 90% [Fig. 4(e)]. A tip radius of ~ 23 nm was determined by comparing Fig. 4(b) with the specifications of the calibration sample.

The presented tuning fork microscope with unglued exchangeable probe and piezotube achieves a performance,

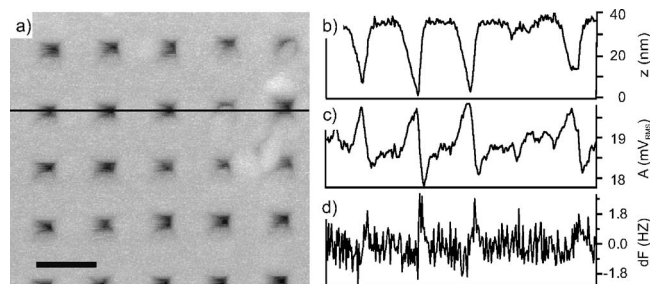


FIG. 4. (a) Shear-force image of a SiO_2 calibration sample (2D200 by Nanosensors, 200 nm scale bar). (b)–(d) Indicated line profile from (a). (b) z : topography signal. (c) A : voltage oscillation amplitude. (d) dF : frequency shift (error signal).

e.g., imaging quality, and approach stability comparable to the best conventionally glued designs. Probe mounting and replacement, as well as mounting of the piezotube, however, is much easier, more reproducible, and extremely fast. The absence of glue will be of particular advantage for operation at nonambient conditions. The adjustability of the Q factor finally allows for an optimal tuning of the feedback loop.

The authors gratefully acknowledge H. -J. Güntherodt for his continuous support and thank J. Y. P. Butter, J. N. Farahani, B. W. Hoogenboom, S. Karotke, A. Lieb, Y. Lill, V. Thommen, and A. Tonin for help and fruitful discussions. Financial support by the Swiss National Science Foundation via the National Center of Competence in Research (NCCR) in Nanoscale Science and a research professorship for one of the authors (B. H.) is gratefully acknowledged.

¹K. Karrai and R. D. Grober, *Appl. Phys. Lett.* **66**, 1842 (1995).

²K. Karrai and R. D. Grober, *Ultramicroscopy* **61**, 197 (1995).

³J. Barenz, O. Hollricher, and O. Marti, *Rev. Sci. Instrum.* **67**, 1912 (1996).

⁴A. G. T. Ruiter, K. van der Werf, J. Veerman, M. F. Garcia-Parajo, W. H. J. Rebsen, and N. F. van Hulst, *Ultramicroscopy* **71**, 149 (1998).

⁵J. Salvi, P. Chevassus, A. Moufard, S. Davy, M. Spajer, D. Courjon, K. Hjort, and L. Rosengren, *Rev. Sci. Instrum.* **69**, 1744 (1998).

⁶D. Mulin, C. Vannier, C. Bainier, D. Courjon, and M. Spajer, *Rev. Sci. Instrum.* **71**, 3441 (2000).

⁷A. Crottini, J. L. Staehli, B. Deveaud, X. L. Wang, and M. Ogura, *Ultramicroscopy* **90**, 97 (2002).

⁸J. Rychen, T. Ihn, P. Studerus, A. Herrmann, K. Ensslin, H. Hug, P. Schendel, and H.-J. Güntherodt, *Rev. Sci. Instrum.* **71**, 1695 (2000).

⁹C. Zilg, R. Mülhaupt, and J. Finter, *Macromol. Chem. Phys.* **200**, 661 (1999).

¹⁰D. Sarid, *Scanning Force Microscopy*, revised ed. (Oxford University Press, New York, 1994).

¹¹R. Stöckle, C. Fokas, V. Deckert, R. Zenobi, B. Sick, B. Hecht, and U. P. Wild, *Appl. Phys. Lett.* **75**, 160 (1999).

¹²K. Karrai and I. Tiemann, *Phys. Rev. B* **62**, 13174 (2000).